Earth and Planetary Science Letters, 109 (1992) 11–23
Elsevier Science Publishers B.V., Amsterdam

[MK]

Sr isotope evolution of seawater: the role of tectonics

Frank M. Richter [a], David B. Rowley [a] and Donald J. DePaolo [b]

[a] *Department of the Geophysical Sciences, University of Chicago, Chicago IL 60637, USA*
[b] *Berkeley Center for Isotope Geochemistry, Department of Geology and Geophysics, University of California, and Earth Science Division, Lawrence Berkeley Laboratory, Berkeley CA 94720, USA*

Received September 25, 1991; revision accepted January 3, 1992

ABSTRACT

We use a high-resolution seawater Sr isotopic evolution curve for the last 100 m.y. in conjunction with modern riverine Sr flux measurements, and also geologic, tectonic and geochronological data, to make the case for a close relationship between seawater Sr isotopic composition and the India–Asia continental collision. Using a simple seawater Sr budget model we begin by showing that the Sr flux associated with alteration of seafloor basalts is too small and does not have the right time evolution to account for much of the seawater Sr isotopic curve of the last 100 m.y. The flux of dissolved Sr carried by rivers originating in the Himalaya–Tibet region on the other hand is presently a significant fraction of the global Sr budget. We calculate how this riverine flux would have had to change with time in order to match the observed seawater Sr isotopic curve and find that the riverine flux remains relatively constant prior to the collision of India with Asia but then increases very significantly after collision. We note that the period of most rapid change in seawater Sr isotopic ratio, from 20 Ma to 15 Ma, is also a period of exceptionally high erosion in parts of the Himalayas and the Tibetan Plateau. As further evidence that Sr derived from the collision of India with Asia plays a major role in the Sr isotopic evolution of seawater we show that the total amount erosion of the Himalaya–Tibetan Plateau since collision, which we calculate separately, represents a total amount of Sr that is very nearly the same as the cumulative amount required by the Sr isotopic change of seawater since collision. The relationship between erosion and riverine Sr flux allows us to use the Sr isotopic evolution of seawater to reconstruct a history of erosion since collision, and we find that the erosion rate accelerates with time since collision, with the present having the largest rate.

When we apply the Sr budget model to the entire Phanerozoic using a new compilation of deformed continental area versus time we find that we can account for the large-scale structure of the seawater Sr isotopic curve, but fail to reproduce several local maxima and minima, especially in the period 100–300 Ma. The present high $^{87}Sr/^{86}Sr$ of seawater and similar highs in the Devonian and Cambrian do correlate with extensive deformation on the continents.

1. Introduction

The $^{87}Sr/^{86}Sr$ of dissolved Sr in seawater, reconstructed for the past 600 m.y. from measurements of marine carbonate sediments [1–6], exhibits well-resolved fluctuations on time scales ranging from hundreds of millions of years [1] to less than one million years [6]. Although the sources of the dissolved Sr in the oceans are reasonably well constrained, there is considerable controversy about the causes of the observed changes in seawater $^{87}Sr/^{86}Sr$ [7–11]. In this paper we focus on the last 100 m.y., and argue that the major cause of the seawater $^{87}Sr/^{86}Sr$ changes is the formation and continuing uplift of the Himalayas and the Tibetan Plateau (hereafter referred to as HTP), and the concomitant increase in the total global weathering rate. In support of this we show that both the timing of collision and the periods of most rapid unroofing of HTP correspond closely to periods of rapid increase in seawater $^{87}Sr/^{86}Sr$, and that the total amount of material removed by erosion from the uplifted areas is approximately the amount of additional erosion needed to explain the overall increase in seawater $^{87}Sr/^{86}Sr$ since 40 m.y. ago. This analysis is facilitated by improvements in the

Correspondence to: Frank M. Richter, Department of the Geophysical Sciences, University of Chicago, Chicago IL 60637, USA.

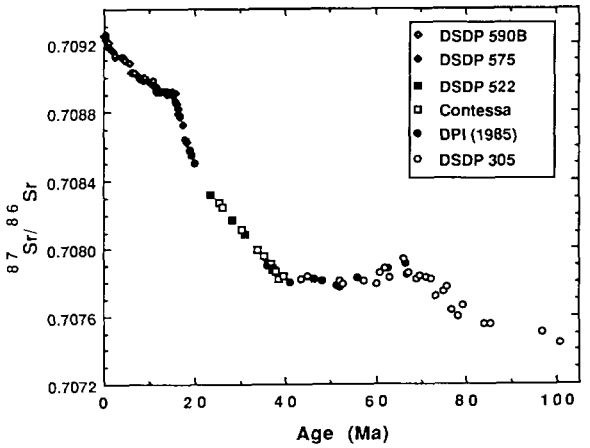

Fig. 1. High-resolution seawater Sr isotopic data for the last 100 m.y. Data sources: DSDP 590B and 575 from Richter and DePaolo [3]; DSDP 522, Contessa and DPI-1985 from DePaolo and Ingram [2]; DSDP 305 from Hess et al. [4].

definition of fine structure in the seawater $^{87}Sr/^{86}Sr$ curve for the last 40 m.y. [2–4,6], recent work on the Sr flux and $^{87}Sr/^{86}Sr$ of major rivers draining the HTP [14], and ^{40}Ar-^{39}Ar studies of unroofing of the HTP [12,13]. We conclude that the primary control on seawater $^{87}Sr/^{86}Sr$ is the amount of dissolved Sr delivered to the oceans by rivers. An additional effect, which may be correlated with the first, is changes in the $^{87}Sr/^{86}Sr$ ratio of the rivers. Both the riverine dissolved Sr flux and the average riverine $^{87}Sr/^{86}Sr$ are mainly a function of the intensity of mountain building via continent–continent collisions.

The data set we use for the seawater Sr isotopic evolution over the past 100 m.y. are displayed in Fig. 1. The curve is constrained to about ± 0.00001 over the past 40 m.y., with the exception of the time period between 19 and 23 Ma where there are more divergent results [15]. For our purposes this is not a major problem; we assume that the curve in this period is a smooth interpolation between the segments immediately preceding and following. For the period from 40 Ma to 100 Ma there are somewhat larger uncertainties, up to ± 0.00005. The most critical part of the curve for our purposes, that covering the last 40 m.y., is well determined by methods that combine high-precision measurements with modelling to correct for the effects of diagenesis [3].

The equations describing the cycling of Sr through the oceans can be found in a number of publications [11,16]. The equations we use are:

$$\mathrm{d}(NR_{sw})/\mathrm{d}t = \sum_n J_n R_n - J_{out} R_{sw} \quad (1)$$

$$\mathrm{d}N/\mathrm{d}t = \sum_n J_n - J_{out} \quad (2)$$

N is the total number of moles of Sr in the ocean, R_{sw} is the $^{87}Sr/^{86}Sr$ of seawater, J_n is the flux of Sr into the oceans from source 'n', which has an average $^{87}Sr/^{86}Sr$ of R_n, and J_{out} is the total flux of Sr out of the oceans. This formulation (eq. 1) contains the approximation that the concentration of total Sr is proportional to the concentration of ^{86}Sr. This is accurate to $\pm 0.01\%$ and hence introduces negligible error. The exact equations are given by Holland [17]. Using eq. (2), eq. (1) can be written as:

$$N\,\mathrm{d}R_{sw}/\mathrm{d}t = \sum_n J_n(R_n - R_{sw}) \quad (3)$$

There are three major fluxes of Sr into the oceans, that carried by rivers (J_r), that due to the hydrothermal alteration of seafloor basalt (J_h), and that due to diagenesis or dissolution of carbonates already on the ocean floor. As shown by Kump [18], the flux due to diagenesis/dissolution is small enough that it can be ignored with no significant lack of accuracy for the purposes of this paper. Thus the equation we work with is:

$$N\,\mathrm{d}R_{sw}/\mathrm{d}t = J_r(R_r - R_{sw}) + J_h(R_h - R_{sw}) \quad (4)$$

The approach is to use the modern measured values of N, R_{sw} and $\mathrm{d}R_{sw}/\mathrm{d}t$, and the estimates available for the modern values of J_r, R_r and R_h [14], to solve for the modern value of J_h. We then assume that R_h is constant and that J_h is proportional to the seafloor generation rate, and use estimates of seafloor generation rate in the past [19] to determine $J_h(t)$. The quantities R_{sw} and $\mathrm{d}R_{sw}/\mathrm{d}t$ as a function of time are derived from the data of Fig. 1. We use a smoothed version of the data for the calculations (Fig. 2). N is typically assumed to be constant and equal to the modern value, although we test for the significance of changes in N to our conclusions. We are thus left with one equation for the value in the past of the quantities J_r and R_r.

The present-day values of N, J_r, R_r, J_h and R_h estimated by Palmer and Edmond [14] are

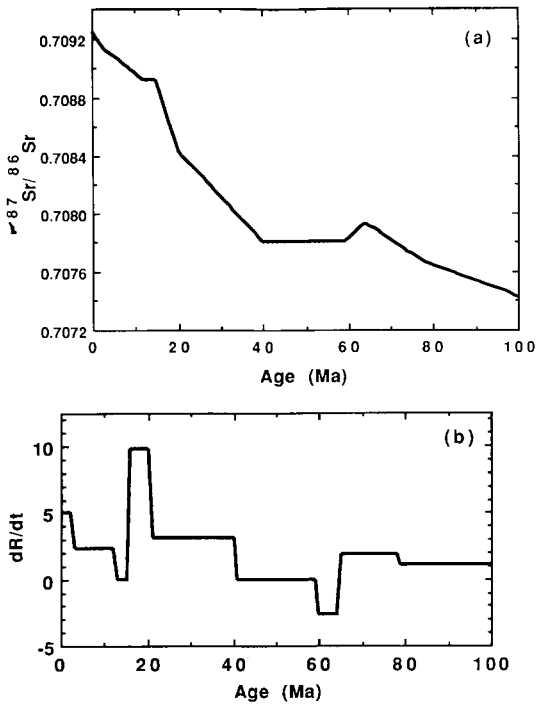

Fig. 2. (a) Sr isotope evolution curve for seawater used in models of the Sr budget of the oceans over the last 100 m.y. (taken from data shown in Fig. 1). (b) Rate of change of the Sr isotopic ratio of seawater taken from (a). Units are change in the 5th decimal place per million years.

given in Table 1, along with the values used in our calculation. The main difference is that we prefer the hydrothermal component to have a Sr isotopic ratio of 0.7030, the typical value for unaltered mid-ocean ridge basalt. The fact that the measured Sr isotopic composition of hydrothermal fluids is typically higher than this results from mixing of Sr from the basalt into a hydrothermal fluid that was originally seawater containing a significant amount of Sr. Since R_h refers to the isotopic composition of new Sr being added to the ocean it should correspond to that of the material being altered. Changing R_h from 0.7035 to 0.7030 results in a slightly lower value for the present-day hydrothermal flux of Sr ($J_h = 0.78 \times 10^{10}$ mol/yr). When we ignore the flux of Sr due to carbonate diagenesis to write eq. (4), we have to use a slightly higher value for J_h ($J_h = 0.82 \times 10^{10}$ mol/yr) for the equation to balance. In general, ignoring the diagenetic flux has the effect of introducing an uncertainty in our determination of the other fluxes of the order of 5%.

TABLE 1

Seawater Sr balance parameters from Palmer and Edmond [14]. Values used in this study that differ from those of Palmer and Edmond are given in parentheses

Total Sr in ocean:	$N = 1.25 \times 10^{17}$ (mol)
River input:	
flux	$J_r = 3.3 \times 10^{10}$ (mol/yr)
isotopic ratio	$R_r = 0.711$
Hydrothermal alteration:	
flux	$J_h = 1.0 \times 10^{10}$ (mol/yr) (0.82×10^{10})
isotopic ratio	$R_h = 0.7035$ (0.7030)
Diagenesis:	
flux	$J_d = 0.3 \times 10^{10}$ (mol/yr) (0)
isotopic ratio	$R_d = 0.7084$

2. Role of hydrothermal alteration

To treat the effects of changing the seafloor hydrothermal flux, the most recent estimates of changes in the seafloor generation rate, $G(t)$, are used [19]. The hydrothermal Sr flux J_h is assumed to be described by $J_h(t) = kG(t)$. Figure 3a shows the results of a model where the riverine flux is kept constant at the present value and the hydrothermal flux is allowed to vary as $G(t)$ from 100 Ma to the present. Figure 3b shows the hydrothermal Sr flux as a function of time in the past corresponding to $G(t)$. The changes in J_h could account for about half of the total change in R_{sw} since 100 Ma; however, the variation with time does not correspond to that observed for the oceans. As shown in Fig. 3a, the effect of $J_h(t)$ is to produce a relatively continuous and featureless change in $^{87}Sr/^{86}Sr$, whereas the actual $^{87}Sr/^{86}Sr$ of seawater is dominated by a rapid rise starting at about 40 Ma.

Figure 3b shows the riverine Sr flux, J_r, that would be needed to reproduce the seawater isotopic evolution given the variation in J_h calculated from the $G(t)$ and the present value of J_h. This calculation assumes a constant value for R_r of 0.711. The riverine flux is required to decrease slightly from 100 Ma to about 40 Ma in response to the decreasing J_h, but starting at about 40 Ma

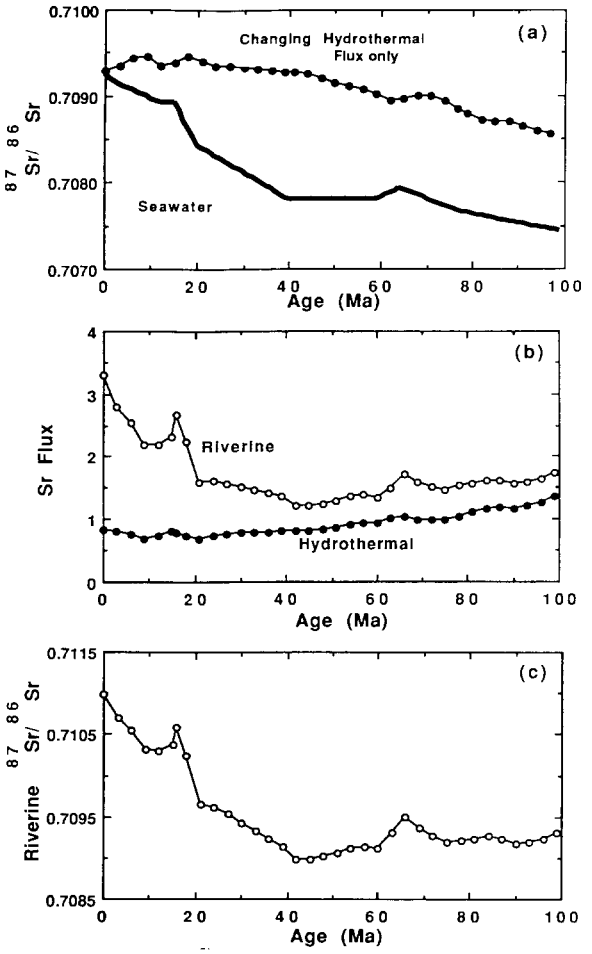

Fig. 3. (a) Calculated seawater Sr isotopic evolution (dots) assuming the hydrothermal flux changes in proportion to the rate of new seafloor generation (dots in Fig. 3b), all other quantities being held at their present-day value (Table 1). The measured Sr isotopic evolution curve is given by the heavy solid curve. (b) Circles are the riverine Sr flux (in units of 10^{10} mol/yr) required by a model calculation that reproduces the measured seawater Sr isotopic evolution curve when the average $^{87}Sr/^{86}Sr$ of river water is held at its modern value of 0.711, and the hydrothermal flux (with $^{87}Sr/^{86}Sr = 0.703$) changes with time in proportion to the rate of of new seafloor generation as shown by the dots. (c) Change in the average $^{87}Sr/^{86}Sr$ of the riverine flux needed to reproduce the measured seawater Sr isotopic evolution curve when the riverine Sr flux is held at its present-day value (3.3×10^{10} mol/yr, $^{87}Sr/^{86}Sr = 0.711$) and the hydrothermal flux varies as shown in (b).

J_r increases substantially. Figure 3c shows how R_r would have to change in order to reproduce the R_{sw} curve when J_r is kept constant at the modern value. These calculations show clearly that the major change in the Sr cycle implied by the seawater isotopic evolution is an increasing flux or ratio of Sr from rivers, commencing at about 40 Ma.

From eq. (4) it can be shown that the fractional change in the calculated riverine flux associated with a change ΔN in the Sr content of the oceans is of the order:

$$\frac{\Delta J_r}{J_r} = \frac{\Delta N \, dR/dt}{J_r(R_r - R_{sw})} \tag{5}$$

In general, changing N is insignificant except when dR/dt is very large. In terms of the calculation of J_r shown in Fig. 3b, the effect of changing N by a factor of two is $\leqslant 5\%$, except for the short period between 20 and 15 Ma when dR/dt is exceptionally large and the effect is about 10%. In particular, decreasing N with increasing age, which could be inferred from the lower Sr concentrations in older fossil material [20], has a negligible effect.

3. The role of tectonics: the India–Asia collision

Raymo et al. [10] cite the increasing R_{sw} value over the past 5 m.y. as evidence of increased erosion and chemical weathering, and hypothesize that rapid erosion of HTP during this time period is responsible. We will use the newer Sr isotopic data for a much longer period of time in conjunction with geologic, tectonic and geochronologic data to argue that the large increase in seawater Sr isotopic composition over the last 40 m.y. is a direct consequence of the collision of India with Asia.

If enhanced weathering associated with the large area of high elevation of HTP contributes significantly to the Sr budget of the oceans, (1) the flux of Sr from rivers draining this region must carry a significant fraction of the total Sr being added to the oceans, (2) the timing of the collision and the onset of increasing J_r or R_r shown in Fig. 3 should occur at much the same time, and (3) the amount of Sr eroded since collision must be sufficient to account for the integrated additional Sr flux required by the R_{sw} curve. In this section we show that all three of these conditions are met. Furthermore, a period of particularly rapid unroofing of HTP between

15 and 20 Ma indicated by new geochronologic data [12,13,21,22] occurs at exactly the time of maximum change in the Sr isotopic composition of seawater (Fig. 2b).

To evaluate the magnitude of the change in riverine flux required by the changing $^{87}Sr/^{86}Sr$ of seawater, it is necessary to isolate first the effect of changing the riverine $^{87}Sr/^{86}Sr$. The data we use for this purpose, taken from Palmer and Edmond [14], are summarized in Table 2. The lower part of the table provides data for major rivers draining the HTP. These data clearly show that requirement (1) above is satisfied—the HTP rivers contribute a significant fraction (at least 25%) of the present total riverine Sr flux. The data also show that the average $^{87}Sr/^{86}Sr$ of the HTP rivers is higher than the average of all other rivers sampled; thus adding an increased Sr flux having the isotopic composition of the HTP rivers will increase the $^{87}Sr/^{86}Sr$ of the global riverine Sr flux. Figure 3c shows the change in R_r needed to account for the increased R_{sw} since 45 Ma, assuming constant J_r of 3.3×10^{10} mol/yr. This increase is approximately 0.002 in $^{87}Sr/^{86}Sr$. Using a value of 0.7127 for the HTP rivers, and taking their contribution to the global Sr flux as 25%, we calculate that in the absence of an increase in J_r the increased $^{87}Sr/^{86}Sr$ of the HTP rivers can account for a change in R_r of less than 0.001, which is no more than about half of that required by the increase in R_{sw} since 40 Ma. We conclude that it is not possible to account for the increase in R_{sw} since 40 Ma by invoking only a change in R_r.

Accordingly, we need a self-consistent model that accounts for both an increased flux and an increased $^{87}Sr/^{86}Sr$ due to HTP rivers in order to isolate the increased Sr flux from the HTP rivers. For this purpose we split the river flux term in eq. (4) into two parts, one to represent the Sr flux (J_{ro}) and isotopic composition (R_{ro}) of rivers other than those draining HTP, and a second part to represent the extra flux (J_{r1}, R_{r1}) needed to explain the observed variations in the isotopic composition of seawater. Equation (4) becomes:

$$N\, dR_{sw}/dt = J_{ro}(R_{ro} - R_{sw}) + J_{r1}(R_{r1} - R_{sw}) + J_h(R_h - R_{sw}) \quad (6)$$

As before, we assume the time dependence of the hydrothermal flux to be given by $G(t)$ times the present hydrothermal flux and that the associated Sr isotopic composition (R_h) is fixed at 0.703. R_{ro} is chosen to approximate the isotopic composition of the Sr flux now provided by rivers other than the HTP rivers ($R_{ro} = 0.710$). J_{ro} is then chosen

TABLE 2

Water flux Q, dissolved Sr concentration, dissolved Sr flux, and Sr isotopic composition for selected rivers from Palmer and Edmond [14]. The first three rivers have the largest water flux and are given for comparing their Sr flux to that of the other rivers listed, which have headwaters in the Himalayan–Tibetan region

	Q (km^3/yr)	Sr (μmol/kg)	Flux (mol/yr)	$^{87}Sr/^{86}Sr$
Amazon	6930	0.32	2.2×10^9	0.7109
Zaire	1250	0.31	0.4×10^9	0.7155
Orinoco	1100	0.21	0.2×10^9	0.7183
Yangtze	900	2.05	1.85×10^9	0.7109
Brahmp.	603	0.93	0.56×10^9	0.7210
Mekong	470	3.39	1.60×10^9	0.7102
Ganges	450	1.58	0.71×10^9	0.7257
Indus	238	3.33	0.79×10^9	0.7112
Irrawady (estimated)	428	3.39	1.45×10^9	0.7102
Salween (estimated)	211	3.39	0.71×10^9	0.7102
		HTP total	7.7×10^9	0.7127
		Global total	3.3×10^{10}	0.711

to satisfy eq. (6) at 100 Ma when J_{rI} is zero ($J_{ro} = 2.2 \times 10^{10}$ mol/yr). Finally, we use $R_{rI} = 0.713$ as an approximation to the present-day average Sr isotopic composition of the HTP rivers. Additional decimal places are not warranted given the actual precision of the data used and the idealized nature of the model calculation.

Figure 4a shows the change in J_{rI} as a function of time needed to produce the observed variation in seawater $^{87}Sr/^{86}Sr$ over the last 100 million years. The model shows that J_{rI} remains near zero from 100 Ma to 40 Ma, which is as it should be if J_{rI} is a consequence of the India–Asia collision. The sustained increase in J_{rI} begins at about 40 Ma, shortly after the collision of India with Asia, and has a total magnitude of the order of 10^{10} mol/yr. This model flux is in reasonably good agreement with the measured flux of dissolved Sr (0.8×10^{10} mol/yr) carried by major rivers draining the HTP, keeping in mind that an inventory for all rivers has not been made. Recall that an increase of about 2×10^{10} mol/yr was required when there is no change in R_r associated with the increased flux (Fig. 3b). Figure 4b shows how the total R_r changes with time in the model as a result of combining the fluxes J_{rI} and J_{r0}, each with a distinctive Sr isotopic composition. There are two local departures from a more or less smoothly varying river flux in Fig. 4a worth noting, one centered at about 65 Ma, the other at about 20 Ma. The older of these may reflect a short-lived increase in the area of deforming continental crust at about 65 Ma (see Fig. 7b) that has nothing to do with the HTP region. The period of high river flux starting at 20 Ma is much more pronounced, and interesting, in that it appears to be associated with a period of particularly rapid unroofing in Tibet [12,13].

Figure 5, taken from [13], shows the data that indicate a period of rapid erosion of the Quxu pluton of the Gandise belt in southern Tibet from about 20 to 15 Ma. There is evidence that this period of rapid unroofing is areally extensive. Zeitler [21] finds a similar increase in the unroofing rates in the far western Himalaya starting at roughly 20 Ma. Also, $^{40}Ar/^{39}Ar$ age determinations on detrital K-feldspars in the Bengal fan made by [22] show a distinct peak in the age distribution at 15–20 Ma. It is quite plausible, then, that the high river fluxes shown in Fig. 4a at

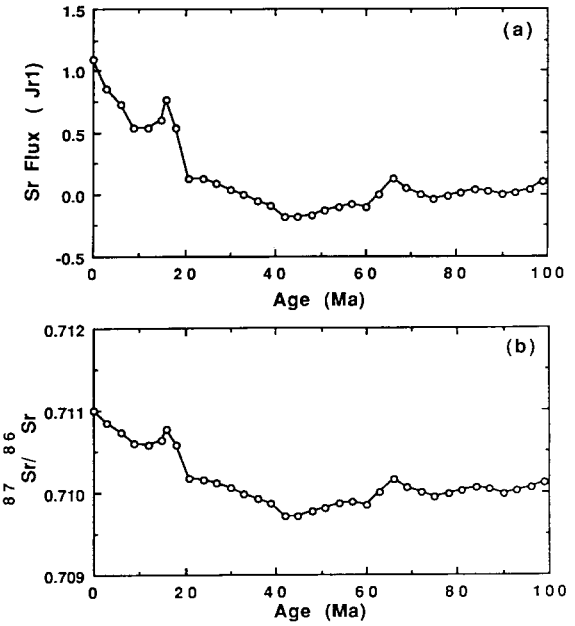

Fig. 4 (a) Additional Sr river flux J_{rI} (flux in excess of a background riverine flux of 2.2×10^{10} mol/yr nee ded for balance at 100 Ma), in units of 10^{10} mol/yr, required to reproduce the seawater Sr isotopic evolution curve when the additional flux has $^{87}Sr/^{86}Sr = 0.713$ (versus 0.710 for the background flux) and the hydrothermal flux, with $^{87}Sr/^{86}Sr = 0.703$, changes in proportion to the rate of generation of new seafloor as shown in Fig. 3b. (b) $^{87}Sr/^{86}Sr$, as a function of time, of the total riverine Sr flux.

15–20 Ma are a reflection of a short-lived unroofing event in Tibet that also affects portions of the Himalayas. Additional data demonstrating that the period of rapid unroofing seen in the Quxu pluton is indeed sufficiently areally extensive to affect the Sr budget of the oceans would be very valuable evidence regarding the provenance of the Sr controlling the $^{87}Sr/^{86}Sr$ evolution of seawater over the last several tens of millions of years.

To evaluate further the connection between the unroofing of HTP and seawater Sr isotopic evolution, we consider in more detail the timing of the collision of India with Asia, and the total amount of erosion that followed. One way of determining the time of collision of India with Asia is to use changes in the relative motion of the two plates involved. The convergence rate should decrease once continental India meets continental Asia and subduction of the intervening oceanic crust ceases. Figure 6 shows the con-

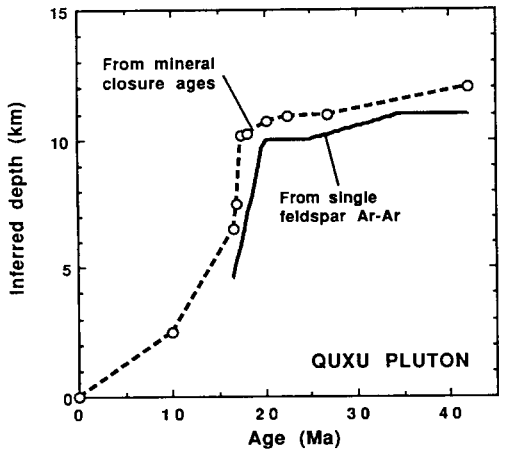

Fig. 5. Unroofing of the Quxu pluton of the Gandgese belt shown in terms of the changing depth of minerals inferred from $^{40}Ar/^{39}Ar$ thermochronometry (from Richter et al. [13]). The heavy solid curve is for a single feldspar sample originally 11 km below the surface at the time of emplacement, while the dashed curve was constructed from data by Copeland et al. [12], who give the age and closure temperature (from which we can infer a depth–age) of minerals sampled at different present elevations. The circles show the depth–age of the individual samples analyzed by Copeland et al. [12] after adjustment to a reference elevation that corresponds to each sample having originated at a depth of 12 km. Both unroofing curves indicate a period of exceptionally rapid erosion beginning at about 20 Ma, which is the same time period during which the most rapid increase in the $^{87}Sr/^{86}Sr$ of seawater occurred (see Fig. 2), and suggests a causal relationship.

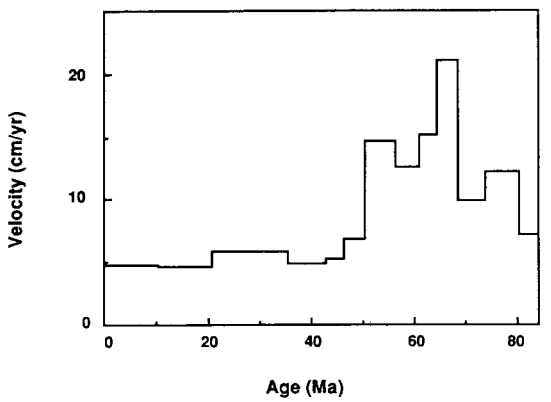

Fig. 6. Plot showing the convergence rate of India (for a point at 27°N,86°E) relative to Asia for the past 84 m.y. constructed using the methods described in Rowley and Lottes [30] and in Pindell et al. [31] applied to all available magnetic anomaly data from the Indian and Atlantic Ocean. We interpret the abrupt decrease in convergence rate at 50 Ma as a reflection of continental India first colliding with the Asian continent.

vergence velocity of India relative to Asia for the past 84 m.y. There is a marked reduction in convergence velocity at 50 Ma which we associate with the initial collision of continental India with continental Asia.

The continued convergence of continental crust during the India–Asia collision has been accommodated in three principal ways: (1) crustal thickening giving rise to the high elevation of the Himalayas and the Tibetan Plateau, (2) erosional removal of some fraction of the crust, and (3) motion along major strike-slip faults which we will refer to as 'tectonic escape'. These processes can be discussed in terms of a general conservation equation for continental crust within a region $\Re$ bounded by the closed curve Σ made up of two segments Σ_1 and Σ_2. Σ_1 lies along the collision zone while Σ_2 encloses a sufficiently large portion of the Asian plate so that all areas of possibly thickened crust due to collision are contained within it. The conservation equation is then:

$$V_{(\Re)} = V_{0(\Re)} + \int_{\Sigma_1}\int_t C_1 \boldsymbol{U}\cdot\boldsymbol{n}\,\mathrm{d}l\,\mathrm{d}t - \int_{\Sigma_2}\int_t C_2 \boldsymbol{U}\cdot\boldsymbol{n}\,\mathrm{d}l\,\mathrm{d}t - \int_{\Re}\int_t E\,\mathrm{d}s\,\mathrm{d}t \qquad (7)$$

which states that the volume $V_{(\Re)}$ of continental crust in $\Re$ at any time t is equal to the initial volume of crust ($V_{0(\Re)}$) plus the cumulative flux of crust of thickness C_1 due to India moving across Σ_1, minus the cumulative loss of crust of thickness C_2 across Σ_2 ('tectonic escape'), minus the cumulative amount of erosion taking place at a rate E over $\Re$. Erosion as used here refers to material that is eroded and removed from $\Re$. In order that the dot product within the first two integrals be positive we have chosen the unit normal $\boldsymbol{n}$ to be into the region $\Re$ along Σ_1 and out of the region along Σ_2.

The conservation equation for crust provides a way of estimating the mean erosion rate of the area since collision of India with Asia if the other quantities in eq. (7) can reasonably assigned. Work by England and Houseman [23] allows for an estimate excess crustal volume ($V_{(\Re)} - V_{0(\Re)} = 1.6 \pm 0.2 \times 10^8$ km^3). The total flux of crust into $\Re$ can be calculated from the relative motion of India relative to Asia (see Fig. 6), an assumed

thickness of the average pre-collisional continental crust (about 35 km) and the time since collision. If as we argued earlier collision began at 50 Ma, the India–Asia convergence represents a total flux of about $2.1 \pm 0.3 \times 10^8$ km^3 of continental crust into $\Re$, the main uncertainty coming from the choice of crustal thickness. Comparing this to the excess crustal volume associated with elevation leads to the conclusion that tectonic escape plus erosion over the past 50 m.y. amounts to about $0.5 \pm 0.35 \times 10^8$ km^3. In the following discussion we will use 0.85×10^8 km^3 as an upper bound on the total erosion of the HTP over the past 50 m.y.

The amount of material eroded and removed from the HTP can also be estimated from the volume of HTP-derived sediments that has accumulated since the middle Eocene. Using isopach maps of the Bengal Fan [24], seismic reflection maps of the Indus Fan [25], and seismic and Airy isostacy-constrained thicknesses of the Makran and Indo-Burman range accretionary complexes, we estimate this volume to be $> 0.4 \times 10^8$ km^3. If it is assumed that the sediment represents 75% of the eroded material, the rest having been carried away in solution [26], the total amount of eroded material is then roughly 0.5×10^8 km^3. We can consider this a lower bound on the amount of material eroded; thus the total volume eroded since collision of India with Asia is between 0.5×10^8 and 0.85×10^8 km^3.

For the model calculations shown earlier to be reasonable we should find that the total amount of erosion since collision can indeed provide enough Sr to support the flux shown in Fig. 4a. Integration of J_{r1} over the last 50 Ma gives 2×10^{17} moles of Sr. The amount of dissolved Sr derived from erosion of the HTP since collision can be calculated by assuming an average concentration of 350 ppm Sr [27] in the 0.5×10^8 to 0.85×10^8 km^3 eroded, 25% of which will be dissolved Sr. The resulting estimate of the total amount of dissolved Sr provided by erosion and weathering since collision is 1.5×10^{17} to 2.4×10^{17} moles, in reasonably good agreement with the estimated excess Sr fluence of 2×10^{17} moles determined from integrating J_{r1} over the last 50 m.y.

Our estimate of 0.5 to 0.85×10^8 km^3 eroded over 50 m.y. corresponds to an average erosion rate of about 0.25 km/m.y. This rate is comparable to the long-term average rate of unroofing of the Quxu pluton (see Fig. 5), but is about an order of magnitude less than the rate during the period of most rapid unroofing, confirming that the rate of erosion in at least a part of the Gandise belt was indeed exceptionally high between 20 and 15 Ma.

The various calculations given above confirm all three of the requirements cited initially. The timing of the India–Asia collisional event, the total erosion of the uplifted mountain belt, and the modern Sr content and $^{87}Sr/^{86}Sr$ of the rivers draining the mountain belt, are all consistent with the requirements of the simple Sr budget model that accounts for the major features of the Sr isotopic evolution of seawater over the past 100 m.y. Furthermore, the correlation in time between an especially rapid increase in the $^{87}Sr/^{86}Sr$ of seawater and a period of very fast unroofing in Tibet at 15–20 Ma also point to Sr from the HTP playing a major role in the Sr budget of the oceans. We conclude that the enhanced erosion associated with the uplift of Himalaya–Tibet, and the high-$^{87}Sr/^{86}Sr$ character of the eroded materials, account for the sustained increase in the marine $^{87}Sr/^{86}Sr$ over the past 40 m.y.

It is noteworthy that the global carbonate sedimentation rate has increased in much the same way as the calculated J_{r1} (Fig. 4b) since 40 Ma [28], with the most dramatic increase coming since 20 Ma. Increased carbonate sedimentation would be predicted from an increased riverine Sr flux, because increased Sr delivery to the oceans should be associated with increased Ca and HCO_3^- delivery, which would lead to enhanced formation of calcium carbonate. Thus the carbonate sedimentation rate is further evidence for an increased rate of global chemical weathering associated with the India–Asia collision, with the largest effect in the last 20 Ma.

4. The Phanerozoic record

The Sr isotopic ratio of seawater during the last 100 m.y. appears to be explained by the mountain-building episode associated with the India–Asia collision. If mountain-building episodes are a general explanation for the structure of the seawater $^{87}Sr/^{86}Sr$-time curve, there

should be a correlation between high $^{87}Sr/^{86}Sr$ and mountain building for the rest of Phanerozoic time. To address this question we need two data bases, the Sr isotope evolution curve from the Cambrian to the present, and some measure of the magnitude of tectonic activity and deformation on the continents as a function of time. For the Sr isotope evolution curve we use data from Burke et al. [1] shown in summary form in Fig. 7a. The measure of continental deformation through time we use is the areal extent of contractional deformation (i.e., that most likely to produce high elevations) resolved in time to the series level (about 20 m.y.).

The areal extent of large-scale contractional continental deformation through time (Fig. 7b) was constructed by measuring the present areal extent of regions showing significant deformation. For each region a time interval for deformation is assigned. Detailed chronologic information is not available for most of the areas, so it is assumed that the area involved was zero at the beginning of the assigned time interval and increased linearly with time to its measured extent by the end of the time interval. A total of 140 separate (in time and/or space) areas of contractional continental deformation were measured. Detailed maps of the areas involved and age assignments will be published separately.

There are at least two reasons why the areas measured are likely to be underestimates. One is that in certain cases it is necessary to extrapolate deformed areas under younger sedimentary cover. This problem is most serious for the West Siberian lowlands, the sedimentary cover of which is presumably underlain by late Early (460–420 Ma) and Late (300–260 Ma) Paleozoic deformed rocks. The lighter curve in Fig. 7b is based on our having estimated the amount of deformed area presently covered and including this additional area in the total plotted. The overall pattern of areal extent versus age is not much changed. Another cause of underestimating the area involved in continental deformation is that some areas will have experienced multiple episodes of deformation, thus modifying the original area involved. We made no effort to palinspastically reconstruct the original areas involved, primarily because we are not able to do so with any confidence. The important point is that while the

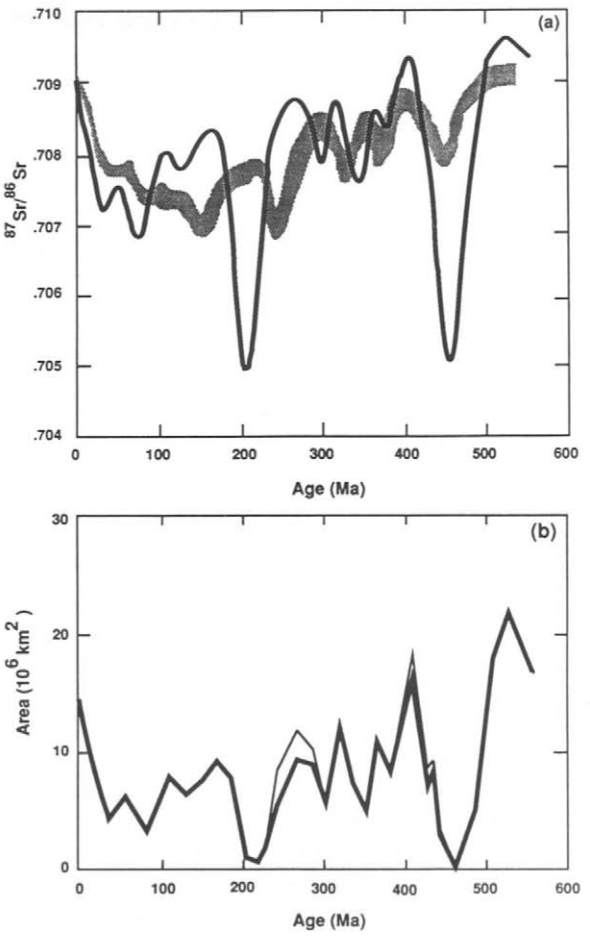

Fig. 7. (a) The Sr isotope evolution curve for seawater since the Cambrian, from Burke et al. [1], shown as a shaded band that encloses 85% of the individual measurements. The continuous curve is the seawater Sr isotopic evolution calculated assuming that the Sr flux carried to the oceans by rivers is a linear function of the area of the continents subject to contractional deformation at any given time. The amount of Sr in the oceans, the isotopic ratio of the river flux, the hydrothermal flux, and its isotopic composition, are all held fixed at their present-day values (Table 1). (b) Minimum and maximum estimates of the areal extent of continental contractional deformation as a function of time plotted using the time scale of Van Eysinga [32]. The minimum areal extent curve was used to calculate the model curve in (a).

actual areas plotted in Fig. 7b may in some cases be uncertain by as much as a factor of two, the timing of the peaks should not be significantly affected.

We use the simplest model to relate continental deformation to Sr isotopic evolution by integrating eq. (4) assuming that the only quantity

that changes in response to continental area deformed is the magnitude of the river Sr flux J_r. We use the following relationship to specify J_r in the past:

$$J_r(t) = 0.75 + 0.0167A(t) \quad (8)$$

where $J_r(t)$ is in units of 10^{10} mol/yr and $A(t)$ is continental area deformed in units of 10^5 km^2. This relationship was determined by comparing deformed area (Fig. 7b) and J_r (Fig. 3b) over the last 40 m.y. The result of integrating eq. (4) over the Phanerozoic, assuming that the river Sr flux obeys eq. (8), is given by the heavy curve in Fig. 7a.

The agreement between the calculated Sr isotope evolution curve and the measured Phanerozoic seawater curve is far from perfect, but the calculated curve captures some of the important aspects of the data. Both records show a general decline in Sr isotope ratios from the present through the Cretaceous followed by a rise to the early Cambrian, and both are characterized by local maxima and minima separated by about 50 m.y. The calculated evolution curve captures three of the most prominent peaks of the actual record: the present high ratio, the high during the Devonian, and the high in the Cambrian. The Late Carboniferous (ca. 300 Ma) peak is however displaced between the model and the record. In the 100 to 240 Ma period there is very poor correspondence between the model and the record. The calculated extreme minima at 200 Ma and 455 Ma are also noteworthy for their lack of correspondence to the record.

Two considerations could bring the model and the record into better agreement. One is the difficulty in assigning ages to the deformational events. The resolution is no better than 20 m.y., and that does not include the difficulty in assessing when stripping by erosion was most pronounced, or in evaluating all of the age information available for the deformational events. Depending on the method used and the materials dated, there could be as much as a 20 m.y. discrepancy between the age we assigned and the actual age. The other consideration is that there are different types of collisional events, which we have not tried to differentiate: Those involving relatively large continental masses composed of thick, old basement rocks, such as the India–Asia event, can produce very thick crust, and expose old and reworked radiogenic basement rocks to erosion at high elevations. Collisions involving the docking of relatively small microcontinents or arc complexes may produce relatively large areas of thin-skinned deformation, but may not generate large areas of high elevation, and the rocks exposed to erosion may be low in $^{87}Sr/^{86}Sr$. In the time period between 240 and 100 Ma there were no major continental collision events; this time period was instead characterized by the docking of a large number of small continental fragments and arc complexes in the circum-Pacific region [29].

The model we have used to relate contractional tectonics to seawater Sr evolution is clearly too simple to capture all the detail of the actual record for the entire Phanerozoic as there must be other factors affecting the Sr isotopic record as well. Nevertheless, we believe we have made an important first step in showing that continental collisional tectonics, and the enhanced erosion and weathering associated with it, are probably the first-order controls on the seawater Sr evolution. Those times when the model fails to fit the data are interesting in the sense that one would like to know whether the data being compared are really adequate, and if they are, what the main additional factor causing the misfit would be.

We can also use the Phanerozoic record to ask whether the present high seawater $^{87}Sr/^{86}Sr$ is in any way exceptional compared to earlier highs. The excess crustal volume presently associated with the high topography of the HTP together with the average rate of erosion estimated earlier can be used to asses how long the present high values of seawater $^{87}Sr/^{86}Sr$ could last into the future. Approximately one-third of the excess crustal volume will be eroded in 50 m.y., if erosion rates remain more or less as they have been over the past 50 m.y. Thus the present pulse of high $^{87}Sr/^{86}Sr$ in seawater could last for another 150 m.y., and perhaps longer if India continues its present convergence with Asia. Compared to the earlier periods of high $^{87}Sr/^{86}Sr$ (see Fig. 7a), all of which (except possibly for the high ending in the Cambrian) lasted less than 100 m.y., the present high seawater $^{87}Sr/^{86}Sr$ seems destined to be exceptionally long lived.

5. Summary and discussion

We tested the proposition that Sr released during large-scale continental deformation, and carried into the oceans by rivers, is the principal forcing factor of seawater $^{87}Sr/^{86}Sr$. The Sr flux due to hydrothermal alteration of seafloor basalt is at present about 25% of the flux due to rivers. Over the past 100 m.y. this flux may have been somewhat larger. If the hydrothermal Sr flux changed in proportion to the rate of production of new ocean crust as estimated by Kominz [19], it will have decreased by about 40% since the Cretaceous, but this change is shown to be too small, and of the wrong shape in time, to account for the the rise in seawater $^{87}Sr/^{86}Sr$ over the last 100 m.y. The cause of the rapid increase in the $^{87}Sr/^{86}Sr$ of seawater that began at 40 Ma is almost certainly due to an increase in the amount of Sr being carried into the oceans by rivers. The required increase in the riverine flux of Sr is about 2×10^{10} mol/yr if the associated Sr isotopic composition is 0.711 (the present average of all rivers), and about 1×10^{10} mol/yr if the associated Sr isotopic composition is 0.713 (the average of the HTP rivers).

We conclude that the cause of the increase in riverine Sr delivery to the oceans since 40 Ma is the collision of India with Asia. In support of this we show the following:

(1) The combined Sr flux of rivers such as the Brahmaputra, Ganges and Indus, with headwaters in the Himalayan–Tibetan region, is of the right order of magnitude and isotopic composition to produce the observed seawater $^{87}Sr/^{86}Sr$ increase since 40 Ma.

(2) The model calculations for the $^{87}Sr/^{86}Sr$ evolution of seawater over the past 100 m.y. require little change in the Sr flux to the ocean in the period preceding the collision of India with Asia, and a sustained increase in the flux beginning shortly after the collision.

(3) Erosion of the HTP since collision provides enough Sr to account for the increased river flux of Sr since collision.

(4) A prominent feature in the timing of the river flux change, a short-lived pulse of high flux starting at 20 Ma, correlates in time almost exactly with a period of exceptionally high erosion in at least some portions of Himalayas and Tibet recorded by $^{40}Ar/^{39}Ar$ thermochronometry.

When we extend our modeling to the entire Phanerozoic we find that the overall shape of the seawater $^{87}Sr/^{86}Sr$ evolution curve and the curve for continental area deformed as a function of time are similar, showing a general decline from the present to about 100 Ma and a general rise from about 100 Ma to 550 Ma. We conclude that continental contractional deformation, and the concomitant increased erosion and weathering, are the primary forcing function for the seawater Sr isotopic composition. On a somewhat shorter time scale there is good agreement between local Sr isotopic ratio highs in seawater and extensive deformation of the continents for the time periods 0 Ma to 100 Ma and 300 Ma to 550 Ma, but from 100 Ma to 300 Ma the Sr isotopic ratios and continental deformation appear to be more nearly anti-correlated. That there is not an exact correlation between the two is not surprising since the elements involved in collisional events vary in both structure and Sr isotopic composition. High seawater $^{87}Sr/^{86}Sr$ ratios reflect continent–continent collisions where old basement rocks are uplifted, partially remobilized, and exposed to extensive erosion. Collisions involving the docking of smaller terranes, many of which are covered with mantle-derived volcanic rocks, would not be expected to increase seawater $^{87}Sr/^{86}Sr$ ratios.

The broader importance of understanding more quantitatively the processes that control the $^{87}Sr/^{86}Sr$ of seawater can be illustrated by calculating an erosional history for the HTP based on the increasing flux of dissolved Sr into the oceans required by the seawater Sr isotopic curve for the last 50 m.y. Our best estimate of this Sr flux as a function of time is given in Fig. 4a. This dissolved Sr flux can be converted back into a source rock volume eroded per unit time by assuming the proportion of eroded Sr that ends up as dissolved Sr (ca. 25% dissolved, 75% detrital), the density of the rock source (ca. 3 g/cm^3), and the concentration of Sr in the source (ca. 350 ppm). The resulting erosion as a function of time is shown in Fig. 8. The uncertainties involved in reconstructing the erosional history of the HTP using seawater Sr are not insignificant, an important source of uncertainty being the actual Sr isotopic composition through time of the Sr flux associated with

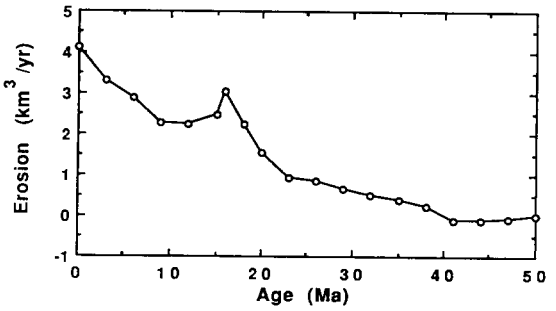

Fig. 8. The erosion rate of the Himalayan–Tibetan Plateau as a function of time that provides the amount of dissolved Sr needed to account for the rise in seawater $^{87}Sr/^{86}Sr$ over the past 50 m.y.

the HTP rivers, which we have fixed at the present value. As seen earlier, there is a direct trade-off between the magnitude of the additional Sr flux required by the increasing $^{87}Sr/^{86}Sr$ of seawater over the last 50 m.y. and the riverine Sr isotopic composition. Keeping in mind that we do have a reasonably good constraint on the total amount of material eroded over the past 50 m.y., we would argue that the erosional history shown in Fig. 8 is resolved to $\pm 30\%$, comparable to the errors in our estimate of the total amount of erosion.

Figure 8 shows a 10 m.y. time lag between the initial collision of India and Asia and increased erosion. This could reflect either a delay in generating the high topography needed for enhanced erosion and weathering, or the fact that a substantial thickness of marine shelf carbonates (with relatively low $^{87}Sr/^{86}Sr$ ratios) needed to be stripped from the emerging highland before exposing the more radiogenic basement rocks. Overall, the erosion rate is seen to accelerate with time, with the present having the largest rate. This need not have been anticipated as one can imagine the alternative that once sufficiently high elevations are produced by the collision the erosion rate would become large and remain so during continued convergence. But this is apparently not the case, which raises the question: why does the erosion rate become progressively larger as a function of time? Is it simply a reflection of an increasing area affected by collision, or does it involve a more complicated interaction between topography and climate? In either case the HTP erosion rate as a function of time since collision shown in Fig. 8 contains important clues as to the nature and timing of the climatic and/or structural consequences of large-scale continental collisions.

Acknowledgements

We thank Mark Harrison for numerous conversations regarding the denudation history of the Himalaya–Tibet region. F.M.R. is supported by National Science Foundation grant EAR 89-17399. D.B.R. is supported by the industrial contributors to the Paleogeographic Atlas Project. D.J.D. is supported by the Director, Office of Energy Research, Office of Basic Energy Sciences, Engineering and Geosciences Division of the U.S. Department of Energy under contract DE-AC03-76SF00098.

References

1 W.H. Burke, R.E. Denison, E.A. Hetherington, R.B. Koepnick, H.F. Nelson and J.B. Otto, Variation of seawater $^{87}Sr/^{86}Sr$ throughout Phanerozoic time, Geology 10, 516–519, 1982.

2 D.J. DePaolo and B.L. Ingram, High-resolution stratigraphy with strontium isotopes, Science 227, 938–941, 1985.

3 F.M. Richter and D.J. Depaolo, Diagenesis and Sr isotopic evolution of seawater using data from DSDP 590B and 575, Earth Planet. Sci. Lett. 90, 382–394, 1988.

4 J. Hess, M.L. Bender and J.-G. Schilling, Evolution of the ratio of strontium 87 to strontium 86 in seawater from Cretaceous to Present, Science 231, 979–984, 1986.

5 J. Hess, L.D. Scott, M.L. Bender, J.P. Kennett and J.G. Schilling, The Oligocene marine microfossil record: age assessments using strontium isotopes, Paleoceanography 4, 655–679, 1989.

6 R.C. Capo and D.J. DePaolo, Seawater strontium isotopic variations from 2.5 million years to the present, Science 249, 51–55, 1990.

7 Z.E. Peterman, C.E. Hedge and H.A. Tourtelot, Isotopic composition of strontium in seawater throughout Phanerozoic time, Geochim. Cosmochim. Acta 34, 105– 120, 1970.

8 R.E. Armstrong, Glacial erosion and the variable composition of strontium in seawater, Nature Phys. Sci. 230, 132–133, 1971.

9 M.R. Palmer and H. Elderfield, Sr isotope composition of seawater over the past 75 Myr, Nature 314, 526–528, 1985.

10 M.E. Raymo, W.F. Ruddiman and P.N. Froelich, Influence of late Cenozoic mountain building on ocean geochemical cycles, Geology 16, 649–653, 1988.

11 D.A. Hodell, P.A. Mueller, J.A. McKenzie and G.A. Mead, Strontium isotope stratigraphy and geochemistry of the late Neogene ocean, Earth Planet. Sci. Lett. 92, 165–178, 1989.

12 P. Copeland, T.M. Harrison, W.S.F. Kidd, X. Ronghua and Z. Yuquan, Rapid early Miocene acceleration of uplift in the Gangdese Belt, Xizang (southern Tibet), and its bearing on accommodation mechanisms of the India-Asia collision, Earth Planet. Sci. Lett. 86, 240–252, 1987.
13 F.M. Richter, O.M. Lovera, T.M. Harrison and P.C. Copeland, Tibetan tectonics from a single feldspar sample: An application of the $^{40}Ar/^{39}Ar$ method, Earth Planet. Sci. Lett., in press, 1990.
14 M.R. Palmer and J.M. Edmond, The strontium isotope budget of the modern ocean, Earth Planet. Sci. Lett. 92, 11–26, 1989.
15 R.C. Capo, Application of strontium isotopes to late Cenozoic paleoceanography and stratigraphy, Ph.D. Thesis, UCLA, 1990.
16 G.W. Brass, The variation of marine $^{87}Sr/^{86}Sr$ during Phanerozoic time: interpretation using a flux model, Geochim. Cosmochim. Acta 40, 721–730, 1976.
17 H.D. Holland, The Chemical Evolution of the Atmosphere and Ocean, Princeton University Press, Princeton, N.J., 1984.
18 L.R. Kump, Alternative modeling approaches to the geochemical cycles of carbon, sulfur, and strontium isotopes, Am. J. Sci. 289, 390–410, 1989.
19 M.A. Kominz, Oceanic ridge volumes and sea level change —an error analysis, Am. Assoc. Pet. Geol. Mem. 36, 109–127, 1984.
20 J. Veizer, Strontium isotopes in seawater through time, Annu. Rev. Earth Planet. Sci. 17, 141–156, 1985.
21 P.K. Zeitler, Cooling history of the NW Himalaya, Pakistan, Tectonics 4, 127–151, 1985.
22 P. Copeland and T.M. Harrison, Episodic rapid uplift in the Himalaya revealed by $^{40}Ar/^{39}Ar$ analysis of detrital K-feldspar and muscovite, Bengal fan, Geology 18, 354–357, 1990.
23 P. England and G. Houseman, Finite strain calculations of continental deformation 2. Comparison with the India–Asia collision zone, J. Geophys. Res. 91, 3664–3676, 1986.
24 J.R. Curray, Possible greenschist metamorphism at the base of a 22-km sedimentary section, Bay of Bengal, Geology 19, 1097–1100, 1991.
25 V. Kolla and F. Coumes, Morphology, internal structure, seismic stratigraphy, and sedimentation of Indus Fan, Am. Assoc. Pet. Geol. Bull. 71, 650–677, 1987.
26 R.M. Garrels and F.T. Mackenzie, Evolution of Sedimentary Rocks, Norton, New York, 1971.
27 K.K. Turekian and K.H. Wedepohl, Distribution of elements in some major units of the Earth's crust, Geol. Soc. Am. Bull. 72, 175–182, 1960.
28 J.R. Southam and W.W. Hay, Global sedimentary mass balance and sea level changes, in: The Sea, Vol. 7, C. Emiliani, ed., pp. 1617–1684, Wiley, 1981.
29 D.B. Rowley, Preliminary Jurassic reconstructions of the Circum-Pacific region, in: IGC Jurassic Circum-Pacific Project, G. Westermann, ed., in press, Cambridge University Press, 1991.
30 D.B. Rowley and A.L. Lottes, Plate kinematic reconstruction of the North Atlantic and Arctic: Late Jurassic to Present, Tectonophysics 155, 73–120, 1988.
31 J.L. Pindell, S.C. Cande, D.B. Pitman, D.B.Rowley, J.F.Dewey, J. LaBrecque and W. Haxby, A plate-kinematic framework for models of Caribbean evolution, Tectonophysics 155, 121–138, 1988.
32 F.W.B. Van Eysinga, Geological Time Scale, 3rd ed., Elsevier, Amsterdam, 1975.